Materials Research Proceedings 41 (2024) 90-99 https://doi.org/10.21741/9781644903131-10

Experimental evaluation of the maximal force before debonding a part from the build platform of an AM printer

SPITAELS Laurent[1,a *], ALDEITURRIAGA OLABARRI Naiara[1,2], BOSSU Julien[1], MARTIC Gregory[3], JUSTE Enrique[3], RIVIERE-LORPHEVRE Edouard[1], ARRAZOLA Pedro-José[2], DUCOBU François[1]

[1] Machine Design and Production Engineering Lab - Research Institute for Science and Material Engineering - University of Mons, Place du Parc 20, Mons, Belgium

[2] Mondragon Unibertsitatea, Loramendi 4, Arrasate-Mondragón, 20500, Spain

[3] Belgium Ceramic Research Centre, Avenue Gouverneur Cornez 4, Mons 7000, Belgium

[a] laurent.spitaels@umons.ac.be

Keywords: Additive Manufacturing, Peel Test, Hybrid Manufacturing, Material Extrusion

Abstract. Hybrid manufacturing relies on the combination of different processes to overcome their own limitations. Combining additive manufacturing such as material extrusion (MEX) and subtractive conventional processes such as milling enables the production of complex design parts with smooth surface and tight tolerances to be foreseen. However, finishing a part directly in the printer by milling operations brings new questions as the maximal force the part can withstand before debonding from the build platform. This paper proposes an experimental method to determine this force by studying the influence of several parameters: the adhesion strategy, the infill pattern and density, the zone of the part where the force is applied as well as the influence of the part design. The method was successfully tested with Polylactic Acid (PLA) parts on a standard MEX printer: the Ultimaker 2+. In the best configuration: no brim, cubic infill of 95% and a force applied on an entire part face, the parts resisted to a force of 50.59 N ± 1.97 N.

Introduction

Additive Manufacturing processes are seen as game changers for the near future [1]. Indeed, from the first developments in the 1980s to 2023, the annual average growth rate of the AM market reached 26.7% [1]. This new way of producing goods begins to be adopted not only for prototyping or modelling, but also now for producing end-user parts [1]. Among the seven families defined by ISO 52900, Material Extrusion (MEX) and Binder Jetting (BJ) are gaining great interest from the industries [2]. They are seen as the two most promising processes in a ten-year horizon for the manufacturing of metallic or ceramics components [2,3]. Indeed, compared to the conventional manufacturing processes (as injection or machining, e.g.), the AM processes enable the production of complex shaped parts which were not possible to achieve before [4]. Moreover, the layer-by-layer nature of AM allows to bring complexity in the material and functions of the parts [4].

However, despite the large progresses achieved in the previous years, the AM processes still lack of capability for producing smooth surfaces with tight tolerances [3–5]. Arithmetic roughness (Ra) values from 9 µm to 40 µm are typical in MEX process [5], while widespread MEX printers produce parts with very large tolerances compared to conventional subtractive processes [6]:

- IT between 12 and 16 of ISO 286-1 for dimensional features.
- L class of ISO 2768-2 for geometrical features.

Post finishing operations (sanding or machining, e.g.) are then required to match the customer specifications [4]. Performing the finishing operations when the part is already totally produced brings new constraints and makes impossible the finishing of complex designs such as lattice, for example. Indeed, the subtractive processes require to access the surfaces to be treated and lack of

flexibility [7]. Moreover, changing of machine to produce and finish the part increases the risk to generate scrap due to wrong part alignments and to the difficulty to take references on very rough surfaces. Therefore, the succession of additive and subtractive operations within the same hybrid machine is seen as a very promising solution to overcome both processes' limitations, while allowing the part production and finishing to be conducted directly on the build platform [1,7,8]. These machines will be able to produce highly customized components at lower cost than each process considered separately [7]. Commercial solutions already exist for the Powder Bed Fusion (PBF) and Directed Energy Deposition (DED) metal AM, but this kind of machines are expensive and requires specific and costly feedstock [7–9]. A more affordable alternative is to use an indirect method such as the MEX of polymers filled with particles of metal or ceramics [9]. In this case, the produced green part does not exhibit the final material properties [10]. It is, therefore, easier to machine and, then, less expensive. Nevertheless, the process is indirect and requires additional operations such as debinding and sintering to obtain a dense part [9]. When the chosen MEX process uses a screw and pellets instead of relying on filament extrusion, the cost savings can be higher. Indeed, Metal Injection Molding (MIM) and Ceramic Injection Molding (CIM) feedstocks exist since decades and can be used in these machines [11]. Furthermore, the knowledge for obtaining the final dense parts by debinding and sintering is already available, while the resulting hybrid machine can be easily integrated into an existing CIM or MIM routes [12].

When foreseeing the use of a hybrid machine, ensuring the adhesion of the part to the build platform is mandatory. Indeed, if the part is finished by milling, it is not clamped but bonded to the build platform. Standards already exist for bonded assemblies (ISO 8510 and ISO 11339), but none can be directly applied to AM parts. Besides, there is still a lack of data for hybrid machines, especially for the maximal forces which can be applied to the part without risking its debonding from the build platform. Many previous papers studied the influence of the printing parameters (infill density and pattern, layer thickness, *e.g.*) on the dimensional accuracy, surface topography and mechanical properties [13]. Only few were dedicated to the analysis of adhesion of the generated roads to the printer build platform [14]. Moreover, the existing studies mainly focus on the influence of the build platform temperature and not on the influence of other printing parameters [14]. This paper aims to close this gap by proposing an experimental method to evaluate the maximal force a part can withstand before debonding from its build platform. Several potential factors of influence are tested, such as the infill pattern and density, the adhesion strategy, the zone on which the force is applied and the part design.

Method

Manufacturing of Parts: The material extrusion printer chosen for the experiments was the Ultimaker 2+. This affordable machine, widespread in many FabLabs and other collaborative workshops, allows to manufacture parts in a set of conventional thermoplastics as PLA (Polylactic Acid), ABS (Acrylonitrile Butadiene Styrene) or even TPU (Thermoplastic Polyurethane). For the tests, the Ultimaker PLA was chosen (material characteristics and properties are available in the datasheet [15]). The printer exhibits a cartesian architecture with a printing volume of 223 mm x 223 mm x 205 mm for its X, Y and Z axes, respectively. The machine was fitted with a 0.4 mm nozzle and uses a standard 2.85 mm diameter filament to produce the parts on its glass build platform.

Three main part designs were used for the experiments as depicted in Fig. 1:

- Geometry A: 20 mm x 20 mm x 20 mm cube with 1 mm radius fillets for its vertical edges;
- Geometry B: a 20 mm x 20 mm x 20 mm cube with 1 mm radius fillets for its vertical edges completed on its top by a cylinder of 15 mm of height and 15 mm of diameter. A 3 mm radius fillet was also added between the cylinder and the cube.

- Geometry C: a 20 mm x 20 mm x 20 mm cube with 3 mm radius fillets for its vertical edges completed on its top by a cylinder of 15 mm of height and 15 mm of diameter. A 3 mm radius fillet was also added between the cylinder and the cube.

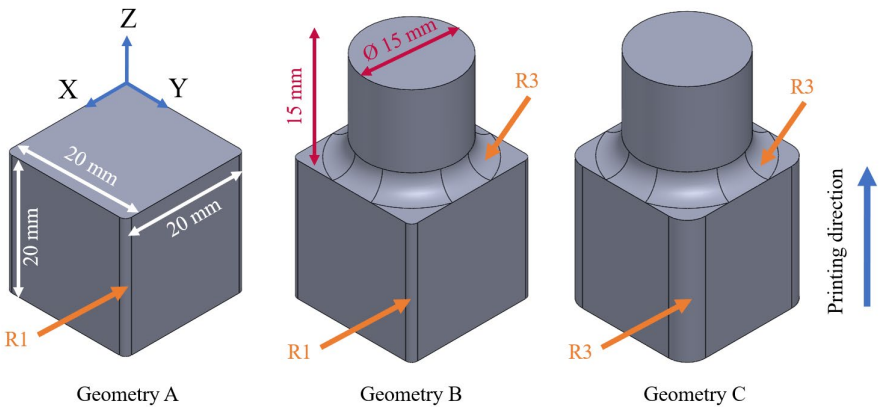

Fig. 1 Three considered part geometries.

These geometries allow to see the influence of the design on the required force a part can withstand before debonding from the build platform. When printed, the cube's faces were oriented with respect to the X and Y axes of the printer. Cura ver. 5.2.1 was used to slice the parts. The printing parameters used to produce the parts are given in Table 1. Two different infill patterns were chosen: cubic and concentric, while three infill densities were tested: 20%, 95% and 100%. The printing direction (as depicted in Fig. 1) was chosen to avoid the need of support structure. No adhesive lacquer (or glue) was used for all the tests. The first layer thickness was set at 0.1 mm (instead of the 0.27 mm standard value in Cura) to ensure a uniform layer thickness throughout the part build direction. The Z offset of the printer was set to 0.1 mm using a gauge.

Table 1 Printing parameters used to produce the parts in PLA with a 2.85 mm filament.

Nozzle diameter	[mm]	0.4
Layer thickness	[mm]	0.1
First layer thickness	[mm]	0.1
Nozzle temperature	[°C]	220
Build platform temperature	[°C]	60
Infill pattern		Cubic or concentric
Infill density	[%]	20, 95 and 100
Adhesive lacquer or glue		No

Experimental plan and setup: The main goal of the experiments was to give an objective measurement of the force a part can withstand before debonding. The force direction of application was set parallel to the build platform since the finishing operations by milling generate mainly forces in this direction.

Three dedicated force application devices (from 1 to 3 as depicted in Fig. 2) were designed to apply a desired force on the part. Two different designs were produced to apply the force on an entire face (Fig. 2.1) of the part or in dedicated zones localized at the build platform level (Fig. 2.2) and part top (Fig. 2.3). The same design (rotated by 180° across its X axis) was used for applying the force at the build platform level and part top. When used, each device was installed on the build platform of the printer around the part to be tested. A nylon wire was attached to the device and linked to a mass using a pulley as depicted in Fig. 3. The pulley can freely turn around its axis, while a dedicated pulley holder linked it to the table on which the printer was installed.

The mass consisted of a plastic can filled of water. The quantity of water was adjustable to obtain the desired level of applied force. In this setup, the friction between the build platform and the force application device was neglected. This indirect force application is necessary due to the reduced accessibility inside the printer.

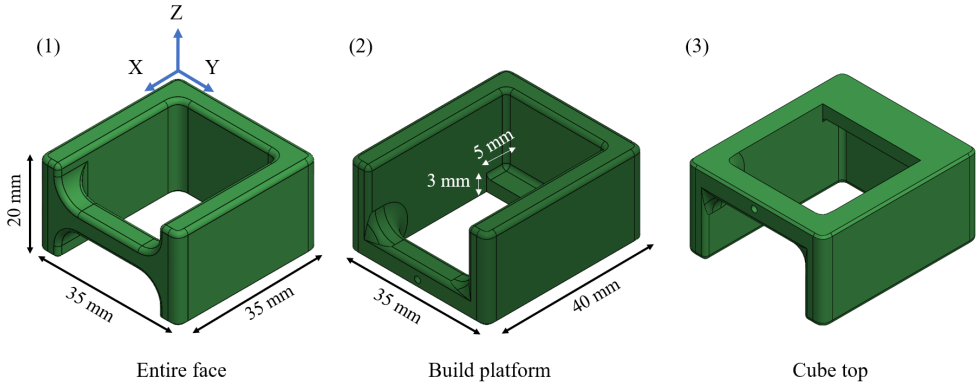

Fig. 2 Devices to apply a force on an entire part face (1), at the build platform level (2) and at the part top (3).

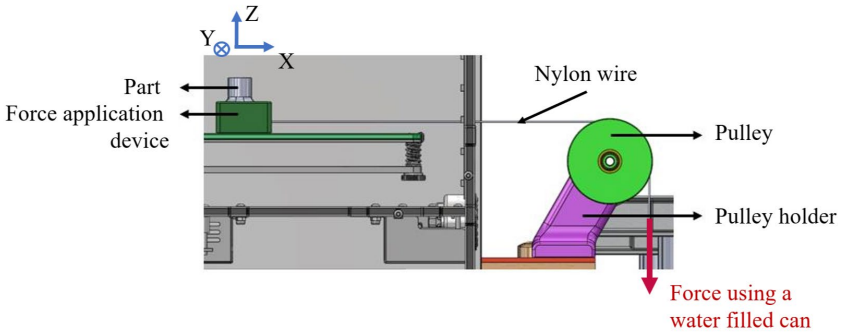

Fig. 3 Application of the force parallel to the X axis via a pulley and a Nylon wire.

Debonding the part can occur in several ways. Indeed, the part can completely peel off the build platform or it can just begin to do so. In both cases, the finishing of the part by a milling operation is compromised. Therefore, a dial gauge with a resolution of 0.01 mm was used to monitor the part debonding directly on the build platform by measuring the part displacement, as depicted in Fig. 4. The dial gauge was installed on a 10 mm slice of extruded polystyrene to insulate it from the build platform. The force applied by the dial gauge rack on the part at the contact point was neglected.

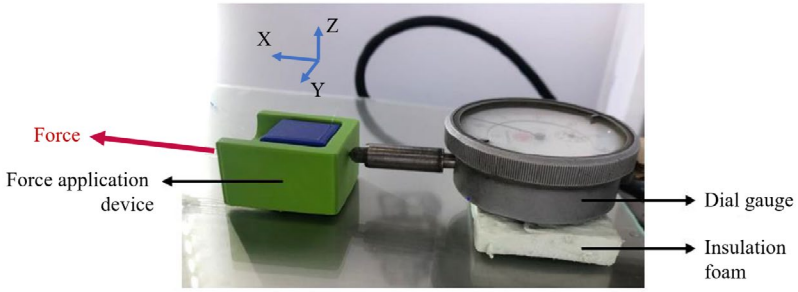

Fig. 4 Monitoring of the part debonding using a dial gauge (resolution: 0.01 mm).

For each of the tests, three repetitions were performed with the same sequence:

- First, the desired part geometry is printed.

- When the print is finished, the build platform temperature is set at the same value as during the printing (60°C) to guarantee having the same conditions as a part finishing performed between two printing operations.
- The force application device is positioned around the part to be tested.
- The dial gauge is then installed in contact with the force application device.
- Five minutes are waited to allow the dial gauge to reach a constant temperature.
- The can, already filled with water to allow a force of 2 N to be applied, is attached to the nylon wire of the setup.
- The force applied is then increased by 1 N every minute by pouring 101,94 mL in the can.
- A part displacement of 1 mm in the dial gauge is the criterion to consider the part debonded from the build platform.

Results

Influence of the Adhesion Strategy: The first tests aimed to compare the effect of using an adhesion strategy or not. Six parts of Geometry A were produced with a cubic infill pattern and 95% of infill. The adhesion strategy selected to be tested was a brim of 8 mm (20 filaments roads). Three parts were printed with the brim and three without, while the force was applied on one entire face. These parameters are summed up in Table 2. The test results are depicted in Fig. 5 with ± σ error bars. The use of a brim was detrimental to the adhesion of the part. Indeed, a nearly 50% higher force can be withstood by the parts without a brim compared with those using this adhesion strategy. During the tests, the brim acted as a weakness point allowing a progressive debonding to occur. Nevertheless, this phenomenon could also result from the part design and the residual stresses it generates. Studying the influence of the part design on the brim efficiency can be an interesting perspective for this work. The repeatability of the tests without brim was also better with a relative standard deviation of 3.9% instead of 10.1% with the brim.

Table 2 Influence of the adhesion strategy - printing parameters.

Part geometry	Geometry A
Infill pattern	Cubic
Infill density [%]	95
Force application zone	One entire face (device 1)
# roads in walls	3
# layers in top/bottom	5
Adhesion by a brim	With and without

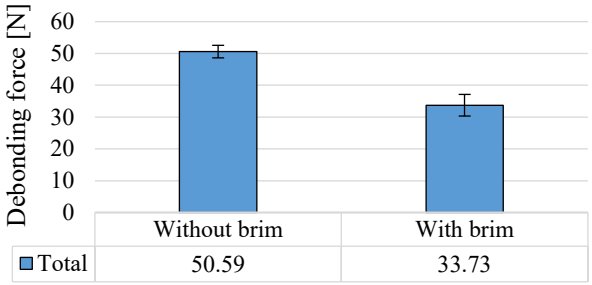

Fig. 5 Influence of the adhesion strategy on the debonding force.

Influence of the Infill Density and Pattern: The influence of the infill density was evaluated by printing three parts with 20% of infill and three others with 95% of infill. The design of the parts was Geometry A, no brim was used, while a cubic infill pattern was selected. The force was applied on one entire face. These parameters are depicted in Table 3. The maximal observed force before debonding is given in Fig. 6. As it can be seen in the graph, higher the infill density, better the

resistance of the part against the applied force. With 95% of infill, a nearly double force was withstood by the parts on average. However, the repeatability of the tests was slightly worse in this case with 4% of relative standard deviation compared to 0.2% in the case of the sparser infill.

Table 3 Influence of the infill density - printing parameters.

Part geometry	Geometry A
Infill pattern	Cubic
Infill density [%]	20 and 95
Force application zone	One entire face (device 1)
# roads in walls	3
# layers in top/bottom	5
Adhesion by a brim	Without

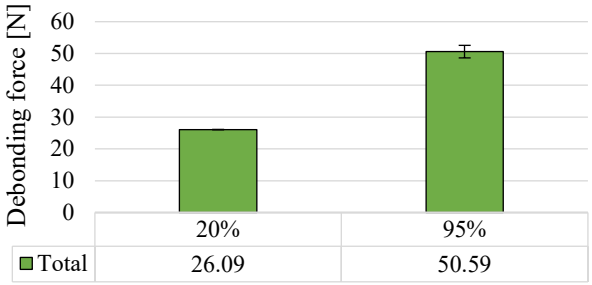

Fig. 6 Influence of the infill density on the debonding force.

The infill pattern was also tested with three other parts using a concentric infill pattern and three others relying on the cubic pattern. All parts were produced with Geometry B, a cubic infill pattern with 100% of infill and the application force on an entire part face as given in Table 4, while the results are given in Fig. 7. As it can be seen, there is an influence of the infill pattern on the force which can be withstood by the part. Indeed, an almost 32.5% higher force can be withstood with the cubic infill pattern compared to the concentric. In terms of repeatability of tests, the cubic infill pattern exhibited slightly better results with a relative standard deviation of 9.5% instead of 14% in the case of the concentric pattern.

Table 4 Influence of the infill pattern - printing parameters.

Part geometry	Geometry B
Infill pattern	Cubic and concentric
Infill density [%]	100
Force application zone	Entire face (device 1)
# roads in walls	0
# layers in top/bottom	0
Adhesion by a brim	Without

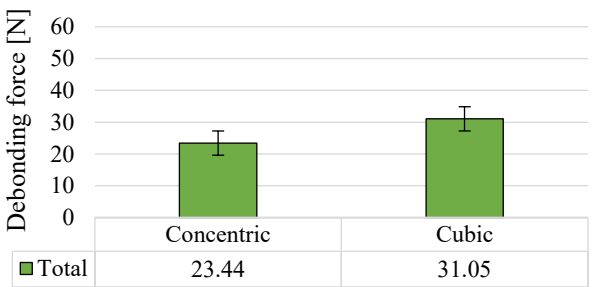

Fig. 7 Influence of the infill pattern on the debonding force.

Materials Research Proceedings 41 (2024) 90-99 https://doi.org/10.21741/9781644903131-10

Influence of the Force Application Zone: The influence of the force application zone was also observed by applying a force on an entire face, at the build platform level and at the top of the cube. For each of the following tests, the part design was Geometry A with a cubic infill pattern and 20% of infill density. The parameters are summed up in Table 5.

Fig. 8, shows the results for each of the configurations. As it can be seen, the highest force is observed for the application point nearer the build platform, followed by the application distributed over an entire part's face. On average the part can endure 55% more force when it is applied the nearest from the build platform. This is logical since a force applied on part's top will generate a torque which will be detrimental to the adhesion of the part. However, even if the application point nearest the build platform led to better average results, it also exhibited the larger relative deviations with up to 13%. Relative deviations of 2.4% and less than 1% were observed for the application zones cube top and entire part's face, respectively. This may come from the temperature of the zone in the vicinity of the build platform. Indeed, a constant temperature of 60°C is maintained for the build platform. The layers in contact with this zone will then be closer to the glass transition temperature of the material, while other zones can reach lower temperatures. However, applying a force at the build platform level may result in unacceptable permanent deformation of the parts due to material softening as shown in Fig. 9a and b.

Table 5 Influence of the force application zone - printing parameters.

Part geometry	Geometry A
Infill pattern	Cubic
Infill density [%]	20
Force application zone	Entire face (device 1)
	Build platform level (device 2)
	Top of the cube (device 3)
# roads in walls	3
# layers in top/bottom	5
Adhesion by a brim	Without

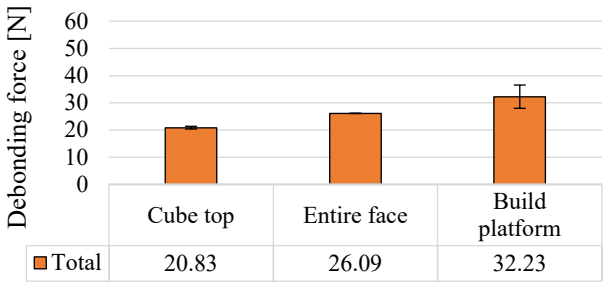

Fig. 8 Influence of the force application zone on the debonding force.

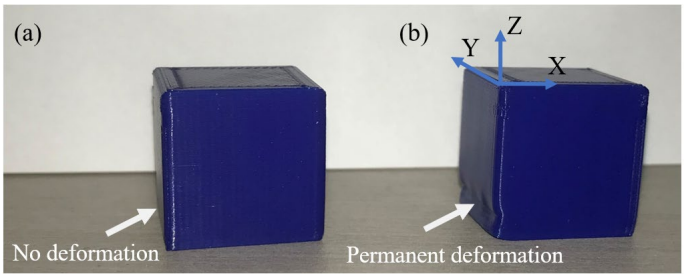

Fig. 9 Parts with a force applied on an entire face (a) and at the build platform level (b).

Influence of the Part Design: The part design can have a strong influence on the residual stresses in the parts [1]. This influence was observed by modifying the design of the parts while keeping all other parameters constant. Geometry A, B and C were considered for the tests. Table 6 gives the printing parameters, while Fig. 10 depicts the results of the experiments.

Geometry A and B can be compared together to highlight the influence of the overall part design (respectively cube or cube + cylinder). As it can be seen, Geometry B resulted in a better adhesion of the part to the build platform with a debonding force 48% higher than Geometry A. This better adhesion may originate from the difference of mass caused by the addition of the cylinder (33% increase of mass) and from the thermal history of the part in the vicinity of the build platform.

Comparing then the results of Geometry B and C allowed to see the influence of the chosen radius filets. Geometry B exhibited fillets radii of 1 mm for its vertical edges, while Geometry C relied on 3 mm radii. The higher radii fillets of Geometry C allowed a 24% higher force to be withstood compared to Geometry B. Moreover, the repeatability was also improved with a relative standard deviation of 3%, 14% and 36% for Geometry C, B and A, respectively. Among the designs, the higher forces were achieved by Geometry C as well as the best repeatability.

The results obtained for the Geometry A in Fig. 10 can be compared to those of Fig. 6. Indeed, the infill pattern and force application zones are identical, while nearly the same infill density was used (95% in Fig. 6 instead of 100% in Fig. 10). However, the results are very different with a maximal force before debonding of 50.59 N and 15.88 N in the case of Fig. 6 and Fig. 10, respectively. This is mostly due to the printing parameters which were different. In Fig. 6, the number of roads for the walls stood at 3, while the bottom and top layers of the part were made of 5 layers. For the tests of Fig. 10, these values were set to zero. This shows a potential strong influence of these printing parameters on the resulting force the part can withstand. However, since the infill density are not identical, no direct conclusion can be drawn. Nevertheless, studying the influence of these parameters can be a perspective of prime interest.

Table 6 Influence of the part design (geometry) - printing parameters.

Part geometry	Geometry A, B and C
Infill pattern	Cubic
Infill density [%]	100
Force application zone	Entire face (device 1)
# roads in walls	0
# layers in top/bottom	0
Adhesion by a brim	Without

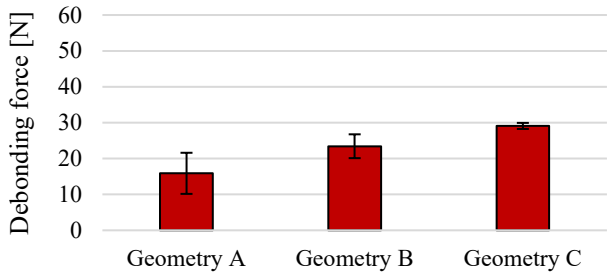

Fig. 10 Influence of the part design (geometry) on the debonding force.

Best Configuration and discussion: The best tested configuration is the following:

- No adhesion strategy (brim).
- A cubic infill pattern with 95% of density.
- A part design of Geometry A.

- A force applied on an entire part face or localized nearer the build platform.
- 3 roads for the walls and 5 layers for the bottom and top layers.

In the perspective of hybrid manufacturing, careful care will be required when foreseeing the finishing of parts produced by the printer directly on its build platform. Indeed, due to the apparition of a torque, applying forces far from the build platform is detrimental to the part adhesion. The process planning for the additive and subtractive operations should then take this observation into account.

Nevertheless, the cutting forces to finish a part made of a thermoplastic composite are relatively low, with level below 15 N [9,16]. Even if the material is not the same, it gives the order of magnitude of the forces during cutting operations. They are lower than the maximal force a part can withstand before debonding. Finish milling operations can then be foreseen.

Conclusions

This paper presented an experimental method to evaluate the maximal force a part can withstand on a build platform just after its printing. This information is of prime interest when planning the finishing of the part directly on the build platform by milling, for example, as in hybrid machines. These are the key findings of the present study:

- In the best tested configuration: no brim, cubic infill of 95%, Geometry A with a force on an entire face, 3 roads for the walls and 5 layers for the bottom and top layers, the parts resisted to 50.59 N ± 1.97 N.
- The use of a brim is detrimental to the adhesion of the part to the build platform. It leads to progressively detach and deform.
- Higher the infill density (95% vs 20%), higher the part adhesion (48% of difference).
- Cubic infill pattern (vs concentric) ensures a 30% higher force to be withstood.
- A force nearer the build platform results in a better part adhesion.
- The part design and, potentially, its resulting residual stresses and thermal history may have an influence on its debonding behavior. However, further measurements (out of the scope of this study) may be required to assess this tendency.
- Higher fillet radii (3 mm instead of 1 mm) for the part edges in contact with the build platform allows 20% higher forces to be withstood.

Perspectives

Comparing the results of the maximal force before debonding with the cutting forces during finish milling of part with the same material is a direct perspective of the work. Assessing the influence of other parameters influencing the part adhesion (build platform texture, number of part wall roads and top and bottom layers) can be also very interesting, while the addition of a thermal camera to the setup could bring some insights about the temperature influence.

References

[1] D. Omidvarkarjan, R. Rosenbauer, C. Klahn, M. Meboldt, Implementation of additive manufacturing in industry, in: E. Pei, A. Bernard, D. Gu, C. Klahn, M. Monzón, M. Petersen, et al. (Eds.), Springer handbook of additive manufacturing, Cham: Springer International Publishing, 2023, pp. 55-68. https://doi.org/10.1007/978-3-031-20752-5_4

[2] Additive Manufacturing Research, Ceramics Additive Manufacturing Markets 2017-2028, an opportunity Analysis and ten-year market forecast, 2018.

[3] S.C. Altıparmak, V.A. Yardley, Z. Shi, J. Lin, Extrusion-based additive manufacturing technologies: State of the art and future perspectives, J. Manuf. Processes 83 (2022), pp. 607-636. https://doi.org/10.1016/j.jmapro.2022.09.032

[4] D. Rosen, Design and Manufacturing Implications of Additive Manufacturing, in: D.L. Bourell, W. Frazier, H. Kuhn, M. Seifi (Eds.), Additive Manufacturing Processes, ASM International, 2020, 24. https://doi.org/10.31399/asm.hb.v24.a0006560

[5] B.N. Turner, S.A. Gold, A review of melt extrusion additive manufacturing processes: II. Materials, dimensional accuracy, and surface roughness, Rapid Prototyp. J. 21 (2015), pp. 250-261. https://doi.org/10.1108/RPJ-02-2013-0017

[6] L. Spitaels, E. Rivière-Lorphèvre, A. Demarbaix, F. Ducobu, Adaptive benchmarking design for additive manufacturing processes, Meas. Sci. Technol. 33 (2022), 064003. https://doi.org/10.1088/1361-6501/ac5877

[7] J. Hafenecker, D. Bartels, C.-M. Kuball, M. Kreß, R. Rothfelder, M. Schmidt, et al., Hybrid process chains combining metal additive manufacturing and forming CIRP J. Manuf. Sci. Technol. 46 (2023), pp. 98–115. https://doi.org/10.1016/j.cirpj.2023.08.002

[8] J.M. Flynn, A. Shokrani, S.T. Newman, V. Dhokia, Hybrid additive and subtractive machine tools - Research and industrial developments, Int. J. Mach. Tool. Manuf. 101 (2016), pp. 79-101. https://doi.org/10.1016/j.ijmachtools.2015.11.007

[9] P. Parenti, S. Cataldo, A. Grigis, M. Covelli, M. Annoni, Implementation of hybrid additive manufacturing based on extrusion of feedstock and milling, Procedia Manuf. 34 (2019) 738-746. https://doi.org/10.1016/j.promfg.2019.06.230

[10] A. Demarbaix, E. Rivière-Lorphèvre, F. Ducobu, E. Filippi, F. Petit, N. Preux, Behaviour of pre-sintered Y-TZP during machining operations: Determination of recommended cutting parameters, J. Manuf. Process. 32 (2018), pp. 85–92. https://doi.org/10.1016/j.jmapro.2018.01.020

[11] V. Martin, J.-F. Witz, F. Gillon, D. Najjar, P. Quaegebeur, A. Benabou, et al., Low-cost 3D printing of metals using filled polymer pellets. HardwareX 11 (2022), e00292. https://doi.org/10.1016/j.ohx.2022.e00292

[12] K. Rane, M. Strano, A comprehensive review of extrusion-based additive manufacturing processes for rapid production of metallic and ceramic parts, Adv. Manuf. 7 (2019), pp. 155–173. https://doi.org/10.1007/s40436-019-00253-6

[13] O. Bouzaglou, O. Golan, N. Lachman, Process Design and Parameters Interaction in Material Extrusion 3D Printing: A Review. Polymers 15 (2023) 2280. https://doi.org/10.3390/polym15102280

[14] M. Spoerk, J. Gonzalez-Gutierrez, J. Sapkota, S. Schuschnigg, C. Holzer, Effect of the printing bed temperature on the adhesion of parts produced by fused filament fabrication. Plast. Rubber Compos. 47 (2018) pp. 17–24. https://doi.org/10.1080/14658011.2017.1399531

[15] Ultimaker PLA Technical data sheet 2022.

[16] L. Spitaels, N. Aldeiturriaga, J. Bossu, G. Martic, E. Juste, P.-J. Arrazola, et al. Tool wear for finishing milling of green thermoplastic-ceramic composites fabricated with pellet AM. Procedia CIRP 121 (2024), pp. 97–102. https://doi.org/10.1016/j.procir.2023.09.235